Supplemental Information

1. Supplemental Figure 1: Comparison of spike waveforms across the experimental session. Relates to Figure 1.
2. Supplemental Figure 2: Quantification of shifter network performance. Relates to Figure 2.
3. Supplemental Figure 3: Test-retest analysis of receptive fields within head-fixed and freely moving recordings. Relates to Figure 3.
4. Supplemental Figure 4: Eye/head position modulation in darkness, and distributions over cell type and layer. Relates to Figure 4.

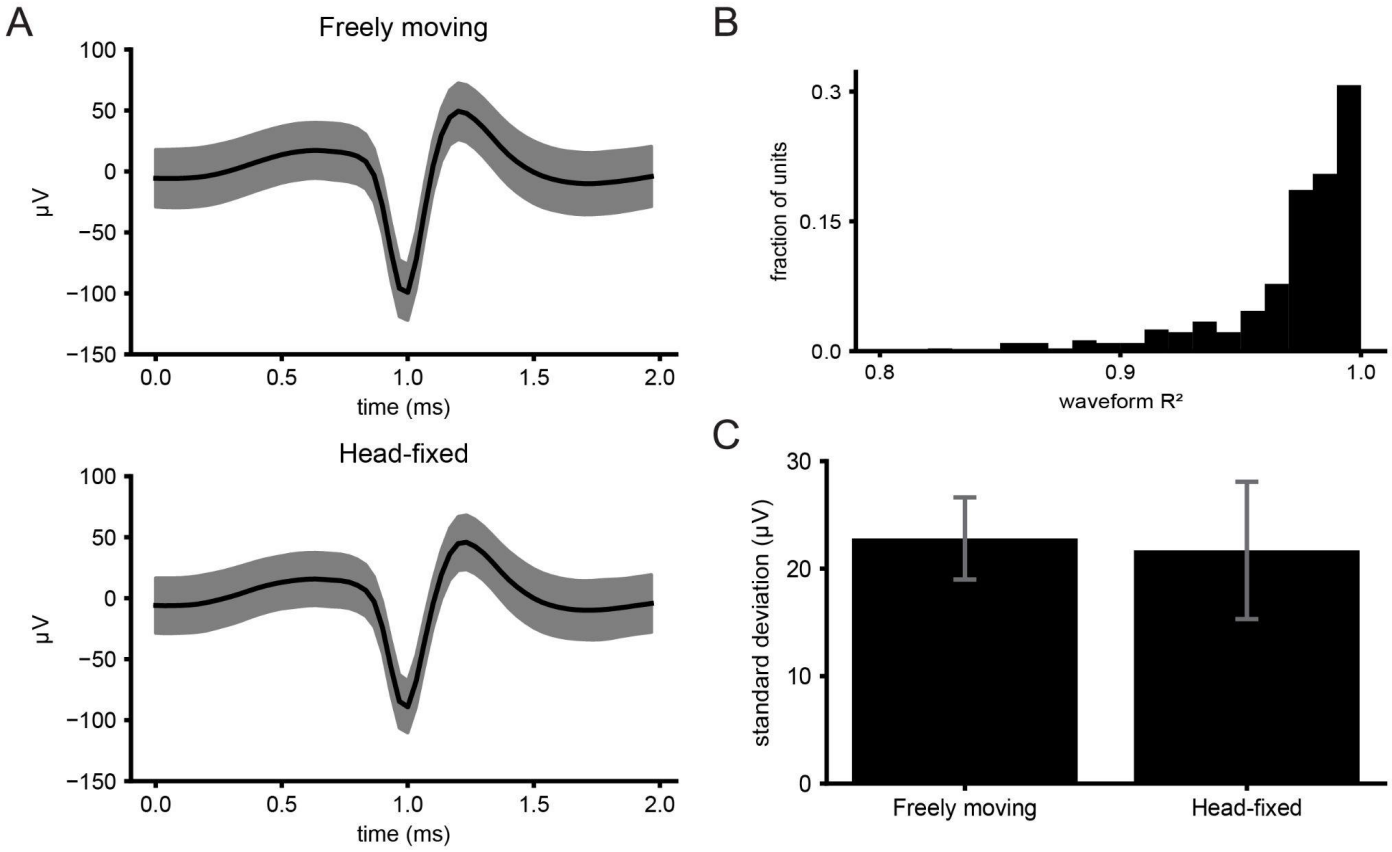

Figure S1: *Comparison of spike waveforms across the experimental session.* **A)** Top: Average spike waveform for one example unit in freely moving recording. Shaded region is one standard deviation. Bottom: Same unit as top but for head-fixed recording of the same unit in the same session. **B)** Histogram of coefficient of determination (R^2) between units of freely moving and head-fixed recordings. **C)** Average standard deviation across 2 ms around spikes for freely moving (FM) and head-fixed (HF) recordings.

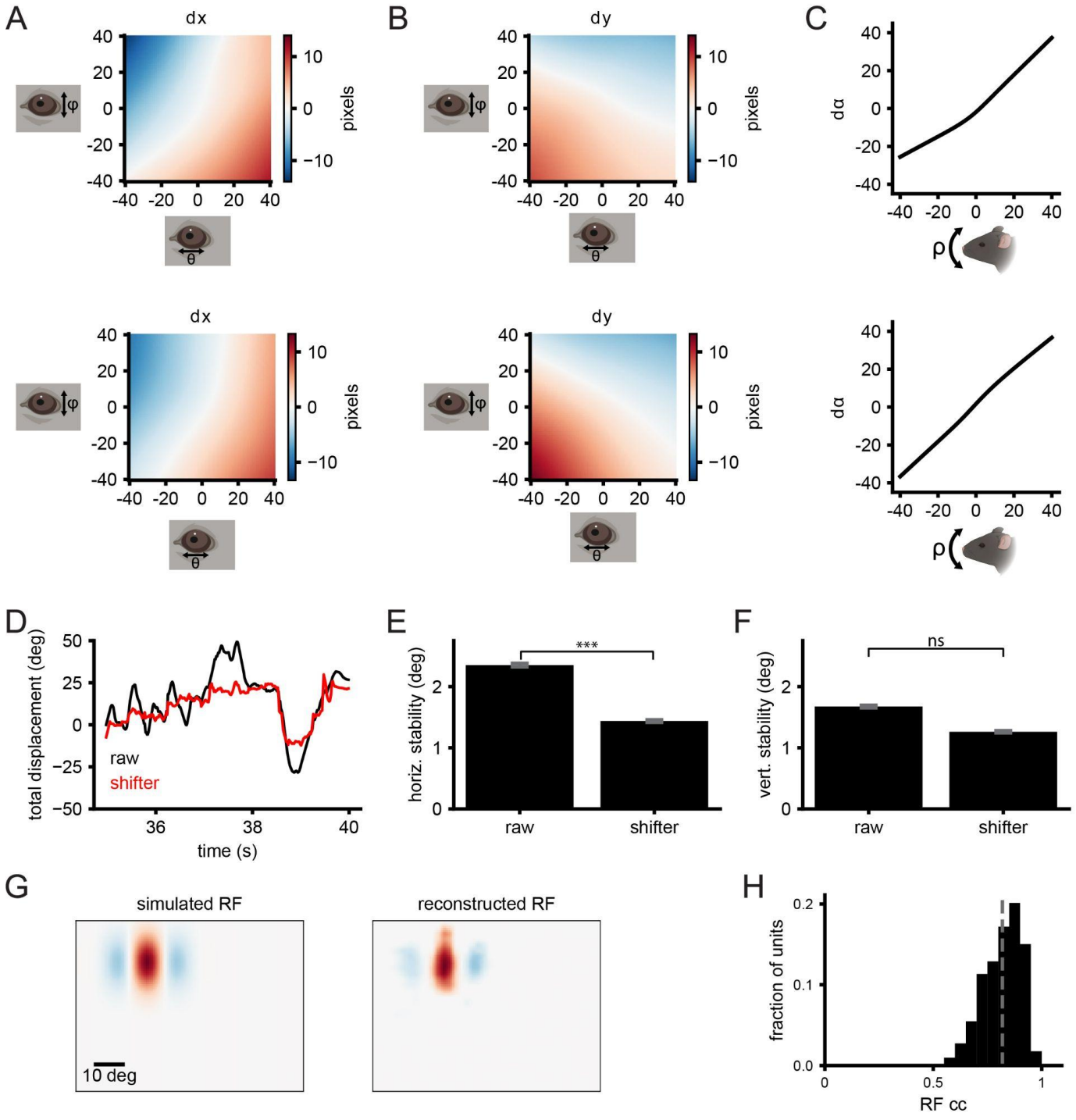

Figure S2: *Quantification of shifter network performance.* **A)** 2-d heat map of horizontal shift for values of theta and phi for first half (top) and second half (bottom) of example recording. **B)** Same as A but for the vertical shift of the image. **C)** Rotation of the image as a function of head pitch for the first half (top) and second half (bottom) of the recording. **D)** Image registration horizontal displacements for shifted and raw world camera video. **E)** Bar plot showing the average horizontal stability of visual angle for compensatory eye movements. **F)** Same as E but for vertical shifts. (***: p-value<0.0013) **G)** Simulated (left) and reconstructed (right) receptive fields with three sub-regions. Same training procedure as Figure 2A. **H)** Histogram of correlation coefficients between simulated and reconstructed RFs. The gray dashed line represents the mean of the distribution.

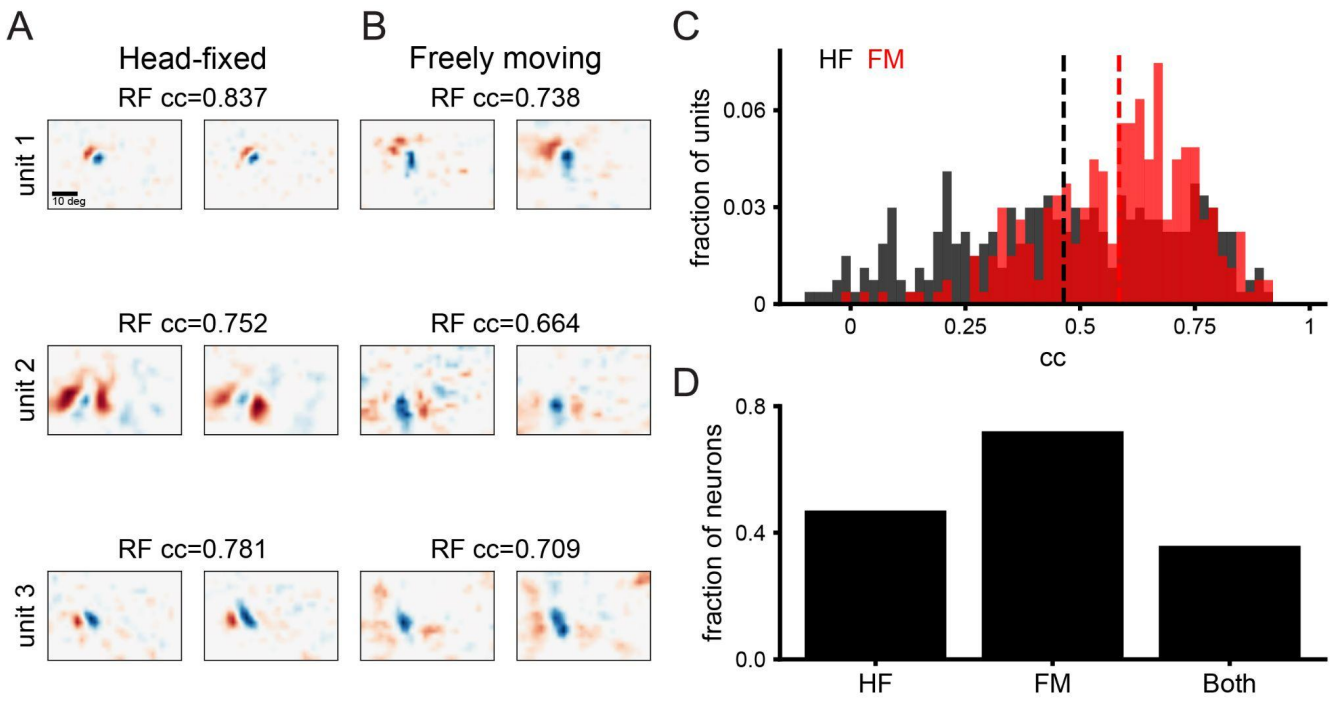

Figure S3: *Test-retest analysis of receptive fields within head-fixed and freely moving recordings.* **A)** Three example receptive fields mapped in the first (left) and second (right) half of a head fixed recording. Correlation coefficient (cc) given is the pixel-wise cc of the receptive fields. **B)** Same as A but for freely moving recording. **C)** Histogram of cc of receptive fields for first versus second half of recording for head-fixed (gray) and freely moving (red) conditions. Dashed lines indicate the mean of the distribution. **D)** Bar plot showing the fraction of units that have a significant cc between the first and second half of the recordings (cc>0.5).

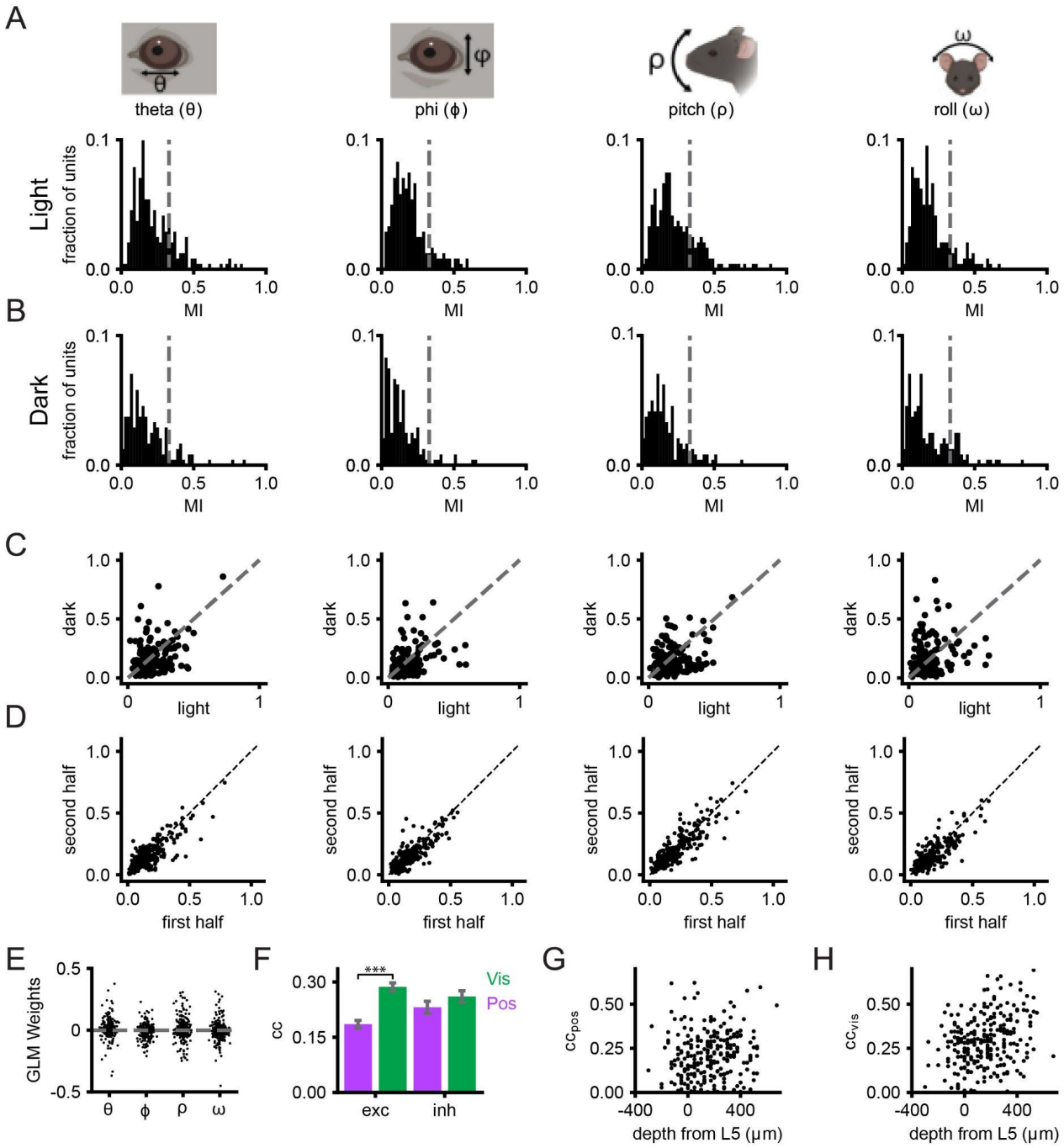

Figure S4: *Eye/head position modulation in darkness, and distributions over cell type and layer. Relates to Figure 4*
A-D) Columns correspond to analyses for theta, phi, pitch and roll respectively. **A)** Histograms of modulation index for single units recorded during free movement in the light. **B)** Same as A but recorded during free movement in darkness. C**)** Scatter plot comparison of light and dark modulation index for each unit. **D)** Modulation index calculated for first half and second half of the freely moving experiments in the light. **E)** Distribution of weights for position only GLM fit for eye/head position. **F)** Correlation coefficient (cc) of predicted versus actual firing rate for visual and position fits split by putative excitatory and inhibitory units. Error bars indicate standard error (***: p-value<0.001, between excitatory visual and position fits). **G)** Correlation coefficient as a function of depth from layer 5 for position fits (>0 deeper, <0 shallower). **H)** Same as G but for visual fits.